IEICE TRANS. COMMUN., VOL.E87–B, NO.6 JUNE 2004

PAPER

Efficient Channel Estimation in DS-CDMA Systems*

Ji-Woong CHOI†, *Student Member and* **Yong-Hwan LEE**†, *Member*

SUMMARY The accuracy of channel estimation significantly affects the performance of coherent rake receiver in DS-CDMA systems. It is desirable for improved channel estimation to employ a channel estimation filter (CEF) whose bandwidth is adjustable to the channel condition. In this paper, we consider the use of moving average (MA) FIR filters as the CEF since it is simple to implement and can provide relatively good receiver performance. First, we optimize the tap size of the MA FIR CEF so as to minimize the mean squared error of the estimated channel impulse response. For practical applications, we propose a low-complexity adaptive channel estimator (ACE), where the tap size of the MA FIR CEF is adjusted based on the estimated channel condition by exploiting the correlation characteristics of the received pilot signal. Numerical results show that the use of the proposed ACE can provide the receiver performance comparable to that of Wiener CEF without exact a priori information on the operating condition.

key words: *adaptive channel estimation, channel estimation filter, DS-CDMA system*

1. Introduction

Coherent detection of DS-CDMA signals requires the channel impulse response (CIR) including the amplitude and phase response of the channel. The CIR is usually obtained by employing a channel estimator, where a lowpass filter, called channel estimation filter (CEF), is employed to reduce the noise effect, improving the accuracy of channel estimation [1]. When a fixed CEF is employed, its cut-off frequency should be large enough to preserve the desired signal whose spectrum is spread to an allowable maximum Doppler frequency. However, if the cut-off frequency of the CEF is much larger than the maximum Doppler frequency of the experiencing channel, the CEF may produce an output with excessive noise, yielding significant performance degradation. This problem can be alleviated by adjusting the bandwidth of the CEF in real time according to the channel condition.

There have been proposed a number of adaptive channel estimation schemes whose parameters can be adjusted in response to the channel condition. The use of least mean square (LMS) adaptation method can be simple, but it may not be effective when the received signal to interference power ratio (SIR) is low [2]. Moreover, since the LMS method has slow convergence property, it may not be applicable to channel estimation when the channel characteristics vary fast. The use of Kalman filters was considered under non-stationary channel condition [3]. However, it requires accurate information on the channel and noise characteristics as well as large implementation complexity, making it difficult to be employed as the CEF in practice. The use of recursive least square (RLS) adaptation method can provide fast convergence, but it requires large implementation complexity and may not be useful for channel estimation when the received SIR is low [4].

In this paper, we consider the use of adaptive MA FIR filters as the CEF since it can easily be designed by simply changing the tap size. Moreover, the MA FIR CEF is simple to implement and can provide relatively good receiver performance if it is properly designed according to the channel condition. Few results have been reported on analytic design of the MA FIR CEF except some simulation results [5], [6]. In this paper, we analytically design the optimum MA FIR CEF by minimizing the mean squared error (MSE) of the CIR.

Even though the optimum tap size of the MA FIR CEF can analytically be designed for a given channel condition, it may not be feasible in practice to implement such an optimum CEF unless the channel condition is known in real time. Recently, there has been proposed a number of adaptive channel estimator (ACE) schemes that employ a simple CEF such as the MA FIR filter [7]–[9]. A simple ACE chooses one of the two CEFs based on the estimated speed of channel variation [8]. The CEF can be selected among multiple CEFs according to the estimated speed zone [7], [9]. Since they consider only non line-of-sight (NLOS) Rayleigh fading with classic spectrum shape, the accuracy of speed estimation may not be acceptable under certain channel condition [7]–[9]. Moreover, since the CEFs are designed in a heuristic manner, their performance may not be improved significantly even if the maximum Doppler frequency is properly estimated.

To mitigate this problem, we design an ACE in an analytic manner. In this paper, we first analytically design the optimum MA FIR CEF by minimizing the MSE of the CIR. Since the maximum Doppler frequency is the most critical factor in determining the bandwidth (i.e., optimum tap size) of the CEF, we estimate it by exploiting the correlation property of the received pilot symbol. To this end, we also analytically derive the optimum tap size of MA CEF as a function of the correlator output. Based on this analytic result, we design an ACE with low-complexity.

Following Introduction, Sect. 2 describes the DS-

Manuscript received May 23, 2003.
Manuscript revised October 29, 2003.

†The authors are with School of Electrical Engineering and Computer Science and INMC in Seoul National University, Seoul, Korea.

*The work was presented in part at the IEEE Vehicular Technology Conference, May 2002.

CDMA system where pilot signal is transmitted in parallel with data signal. The optimum MA FIR CEF is analytically designed by minimizing the MSE of the CIR in Sect. 3. In Sect. 4, we propose an ACE that adjusts the bandwidth of the CEF by estimating the channel condition in real time. The receiver performance of the DS-CDMA system with the use of the proposed ACE is verified in Sect. 5. Finally, conclusions are summarized in Sect. 6.

2. DS-CDMA System with a Pilot Channel

We consider a DS-CDMA system that transmits a pilot signal in parallel with user signals [10], [11]. Since a common pilot signal can be transmitted with a large transmit power in the downlink, the channel information can be more accurately estimated than in the uplink. As a result, we consider the channel estimation problem in the uplink. Note that the design of the channel estimator for the uplink can also be applied for the downlink.

In the transmitter of user-i, the user data is first convolutionally encoded with code rate C and constraint length H, and then interleaved. We omit the user index i for ease of description. Assume that the data and pilot signal are transmitted together through the real and imaginary path, respectively [10], [11]. Letting β^2 be the pilot to data signal power ratio (PDR), a baseband equivalent transmit signal $x(t)$ can be represented as

$$x(t) = \sum_{k=-\infty}^{\infty} \sum_{n=0}^{N-1} g[k] \Big(x_d[k] w_d[kN+n] + j\beta x_p[k] w_p[kN+n] \Big) q[kN+n] p_{T_c}(t - nT_c) \tag{1}$$

where N is the spreading factor (SF), T_c is the chip duration interval, T is the symbol duration time equal to NT_c, $x_d[k]$ is the user message symbol having an amplitude equal to 1 or -1 at time $t = kT$, $x_p[k]$ is the pilot symbol having an amplitude equal to 1, $w_d[n]$ and $w_p[n]$ are bipolar orthogonal spreading sequences allocated to the data and pilot signal, respectively, $g[k]$ is the gain of the k-th symbol employed for fast power control (FPC), $p_{T_c}(t)$ is a unit-amplitude rectangular pulse defined in $[0, T_c]$ and $q[n]$ denotes a user specific complex PN scrambling sequence with $|q[n]| = 1$.

Assuming that there are L independent propagation paths with different channel gain and time delay, the CIR of the channel $h(t, \tau)$ at time t can be represented as

$$h(t, \tau) = \sum_{l=0}^{L-1} h_l(t) \delta(\tau - \tau_l) \tag{2}$$

where $\delta(\tau)$ is Dirac delta function and τ_l is the delay of the l-th path signal. The CIR $h_l(t)$ of the l-th path can be represented by

$$h_l(t) = \alpha_l(t) e^{j\phi_l(t)} \tag{3}$$

where $\alpha_l(t)$ and $\phi_l(t)$ are the amplitude and phase response of the l-th path at time t, respectively. We assume that the amplitude $\alpha_l(t)$ is Ricean distributed with Ricean factor K_l and $\phi_l(t)$ is uniformly distributed over $[0, 2\pi]$ [12]. Denoting P_l and θ_l by the power and arrival angle of the specular component, and $\sigma^2_{\alpha,l}$ by the average power of the scattered component, K_l is equal to $P_l \sigma^{-2}_{\alpha,l}$. As a special case, the channel becomes a Rayleigh fading channel when K_l is zero.

The received signal $r(t)$ can be expressed by

$$r(t) = \sum_{l=0}^{L-1} h_l(t) x(t - \tau_l) \ + n(t) \tag{4}$$

where $n(t)$ denotes the total interference term composed of the background noise, self interference from the desired user, and other users' interference from the desired and adjacent cells. Assuming that the number of users is not too small, $n(t)$ can be approximated as additive white Gaussian noise (AWGN) with zero mean and two sided power spectrum $I_0/2$ [13]. Assuming that there are F fingers in the rake receiver, the output of the rake receiver with the maximal ratio combining (MRC) can be represented as

$$\hat{y}[k] = \sum_{l=0}^{F-1} y_l[k] \tag{5}$$

where $y_l[k]$ is the output of the l-th finger at time $t = kT$ given by

$$y_l[k] = \mathrm{Re} \left\{ \int_{kT}^{(k+1)T} r(t + \tau_l) c_d^*(t) \hat{\alpha}_l[k] e^{-j\hat{\phi}_l[k]} dt \right\}. \tag{6}$$

Here, $\hat{\alpha}_l[k]$ and $\hat{\phi}_l[k]$ are respectively the estimated amplitude and phase of the channel at time $t = kT$, the superscript * denotes the complex conjugate and $c_d(t)$ is the data spreading signal represented as

$$c_d(t) = \sum_{n=-\infty}^{\infty} q[n] w_d[n] p_{T_c}(t - nT_c). \tag{7}$$

The instantaneous CIR can be acquired from the pilot symbol by

$$\begin{aligned} \tilde{h}_l[k] &= \frac{-j}{\beta T} \int_{kT}^{(k+1)T} r(t + \tau_l) c_p^*(t) dt \\ &= g[k] \alpha_l[k] e^{j\phi_l[k]} + \frac{1}{\beta} n_l[k] \end{aligned} \tag{8}$$

where $c_p(t)$ is the pilot spreading signal expressed by

$$c_p(t) = \sum_{n=-\infty}^{\infty} q[n] w_p[n] p_{T_c}(t - nT_c) \tag{9}$$

and $n_l[k]$ is AWGN with zero mean and variance $\sigma^2_{n,l}$ equal to $I_{0,l}/T$ ($=\xi_l I_0/T$), where

$$I_0 = \frac{1}{L} \sum_{l=0}^{L-1} I_{0,l}. \tag{10}$$

Here, ξ_l varies according to the spreading sequence and channel condition such as the time-delay profile. We assume that all the fingers suffer from same interference power on the average, i.e., ξ_l is equal to one.

3. Optimum MA FIR CEF

We design the optimum MA FIR CEF assuming that the large-scale fading is perfectly compensated by slow power control (SPC) and the small-scale fading effect is only remained in the received signal, i.e., $g[k]$ is constant (=1). When a $(2M_l + 1)$-tap MA filter is employed as the CEF of the l-th finger, the CIR of the l-th path can be estimated by

$$\begin{aligned}\hat{h}_l[k] &= \frac{1}{2M_l+1}\sum_{i=-M_l}^{M_l}\tilde{h}_l[k+i] \\ &= \frac{1}{2M_l+1}\sum_{i=-M_l}^{M_l}\left(h_l[k+i]+\frac{1}{\beta}n_l[k+i]\right). \end{aligned} \tag{11}$$

We design the MA FIR CEF so as to minimize the MSE of the estimated CIR. Note that the optimum tap size minimizing this MSE also minimizes the BER performance [14]. Define $\varepsilon_l[M_l]$ by the MSE of the l-th path channel estimator

$$\varepsilon_l[M_l] = E\left\{\left|\hat{h}_l[k]-h_l[k]\right|^2\right\} \tag{12}$$

where $E\{x\}$ denotes the ensemble average of x. It can easily be shown that the MSE is represented as

$$\begin{aligned}\varepsilon_l[M_l] &= R_{h,l}[0]+\frac{1}{(2M_l+1)^2}\sum_{i=-M_l}^{M_l}\sum_{j=-M_l}^{M_l}R_{h,l}[i-j] \\ &\quad -\frac{2}{2M_l+1}\sum_{i=-M_l}^{M_l}R_{h,l}[i]+\frac{1}{2M_l+1}\frac{\sigma_{n,l}^2}{\beta^2}\end{aligned} \tag{13}$$

where $R_{h,l}[i]$ is the real part of autocorrelation of the l-th sampled impulse response defined as

$$R_{h,l}[i] = E\left\{\mathrm{Re}\left(h_l^*[n]h_l[n+i]\right)\right\}. \tag{14}$$

By changing the summation form in (13) into an integral form, the MSE can be approximated by

$$\begin{aligned}\varepsilon_l(\kappa_l) &\approx R_{h,l}(0)+\frac{1}{(2\kappa_l)^2}\int_{-\kappa_l}^{\kappa_l}\int_{-\kappa_l}^{\kappa_l}R_{h,l}(t-u)dtdu \\ &\quad -\frac{1}{\kappa_l}\int_{-\kappa_l}^{\kappa_l}R_{h,l}(t)dt+\frac{T}{2\kappa_l}\frac{\sigma_{n,l}^2}{\beta^2} \\ &= R_{h,l}(0)+\frac{1}{2\kappa_l^2}\int_0^{2\kappa_l}R_{h,l}(t)(2\kappa_l-t)dt \\ &\quad -\frac{2}{\kappa_l}\int_0^{\kappa_l}R_{h,l}(t)dt+\frac{T}{2\kappa_l}\frac{\sigma_{n,l}^2}{\beta^2}\end{aligned} \tag{15}$$

where κ_l is equal to $(M_l + 1/2)T$ and $R_{h,l}(\tau)$ is the autocorrelation of the impulse response of the l-th path channel given by

$$\begin{aligned}R_{h,l}(\tau) &= E\left\{\mathrm{Re}\left(h_l^*(t)h_l(t+\tau)\right)\right\} \\ &= P_l\cos(2\pi f_d\tau\cos\theta_l)+\sigma_{\alpha,l}^2R_{\alpha,l}(\tau).\end{aligned} \tag{16}$$

Here, f_d denotes the maximum Doppler frequency and $R_{\alpha,l}(\tau)$ is the autocorrelaton of scattered components in the l-th path signal given by [12]

$$R_{\alpha,l}(\tau) = \begin{cases} J_0(2\pi f_d\tau), & \textit{Classic spectrum} \\ \frac{\sin(2\pi f_d\tau)}{2\pi f_d\tau}, & \textit{Flat spectrum}\end{cases} \tag{17}$$

where $J_0(\cdot)$ is the first kind, zero-th order Bessel function.

Using the optimum κ_l minimizing $\varepsilon_l(\kappa_l)$, the optimum tap size $\hat{N}_l$ (=$2\hat{M}_l$+1) can be determined as (refer to Appendix A)

$$\begin{aligned}\hat{N}_l &= 2\hat{\kappa}_l/T \\ &= \left\{\frac{1}{(\pi f_dT)^4C\gamma_{b,l}S_l\beta^2}\cdot\frac{1+K_l}{K_l\cos^4\theta_l/9+1/\chi_l}\right\}^{1/5}\end{aligned} \tag{18}$$

where $\gamma_{b,l} = E_b/I_{0,l}$, χ_l is a constant equal to 24 and 45 in the case of the classic and flat spectrum, respectively, and S_l is the ratio of the l-th path signal power to total signal power

$$S_l = \left(P_l+\sigma_{\alpha,l}^2\right)\Big/\sum_{i=0}^{L-1}(P_i+\sigma_{\alpha,i}^2). \tag{19}$$

Note that $\hat{N}_l$ decreases as f_d, $\gamma_{b,l}$, β^2, K_l and/or S_l increase and it is most influenced by f_d.

In practice, the transmit signal is fast power controlled in a DS-CDMA system to compensate the fast fading as well as the near-far effect [1]. However, most of studies on channel estimation have assumed the use of SPC and few results have been reported with the use of FPC. Since the FPC includes time-varying nonlinear feedback process, it would be useful for design of the channel estimator if the effect of the FPC can be approximated by a simple model.

Figure 1 compares the analytic design (18) with the simulation result in Rayleigh (K_l=0) fading channels with a classic spectrum, when T = 1/19200 sec, β^2= 1/4, C = 1/2, χ_l= 24 and $\gamma_{b,l}$ = 5 dB, where 'simulation' denotes the tap size minimizing the MSE (12) obtained by computer simulation. Here, we assume a three-path channel with the same channel gain and interference power on the average. We also assume that the SIR is perfectly estimated and that the power control is performed with a step size of 1 dB at a rate of 800 Hz without any error. It can be seen that the optimum tap size is almost the same irrespective of the use of SPC and FPC except for small f_d. This implies that the correlation property of the received signal is little affected by the use of fast power control unless f_d is small. Note that fast power control adjusts the real-valued gain $g[k]$, affecting only the power of the received signal, but not the phase. Note also that if f_d is small, the FPC can cause the transmit signal to have fluctuation in the magnitude at a rate higher

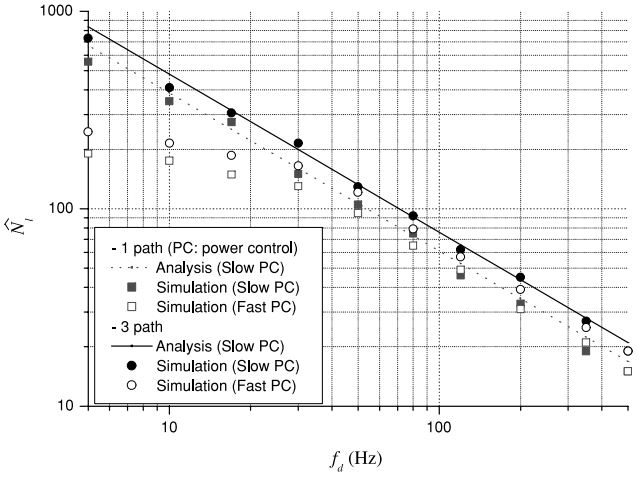

Fig. 1 Optimum MA FIR CEF tap size in Rayleigh fading channel.

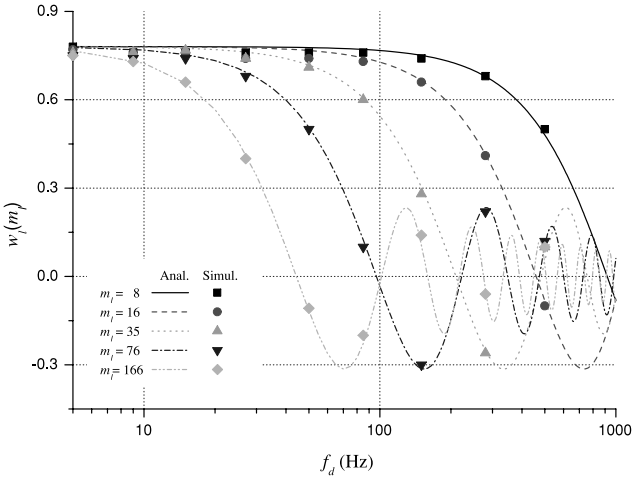

Fig. 2 The output of the correlator bank.

than f_d, resulting in the increase of high frequency term in the power spectral density of the received pilot signal. As a result, the design of the optimum MA FIR CEF can also be applied to the use of FPC unless f_d is small. For small f_d, it may be practical to fix the tap size of the MA FIR CEF since the optimum tap size is slightly changed as seen in Fig. 1.

4. Proposed Channel Estimator

For a given f_d, the optimum tap size $\hat{N}_l$ decreases as β^2, $\gamma_{b,l}$, K_l, C and/or S_l increase, and vice versa. However, since these parameters have less effect on $\hat{N}_l$ than f_d, the optimum tap size is not significantly affected by the variation of these parameters other than f_d. Moreover, the variation of the tap size can further be reduced since β^2 and C are usually predetermined in practice. Thus, if f_d is correctly estimated, the tap size can be determined without significant performance degradation even when other channel condition parameters are not known.

It may not be easy to accurately estimate f_d with low complexity under various channel conditions [7], [8], [15], [16]. The maximum Doppler frequency f_d can be estimated by exploiting the correlation function of the received pilot signal over J symbols,

$$w_l(m_l) = \frac{\sum_{k=0}^{J-1} \mathrm{Re}\{\bar{h}_l^*[k]\bar{h}_l[k+m_l]\}}{\sum_{k=0}^{J-1} \left|\bar{h}_l[k]\right|^2} \tag{20}$$

where $\bar{h}_l[k]$ is pre-filtered output of $\tilde{h}_l[k]$ to suppress the noise components larger than the allowable maximum Doppler frequency. For simplicity of design, we consider the use of an N_a-tap MA FIR filter as the prefilter.

Figure 2 depicts $w_l(m_l)$ for five different values of m_l as a function of f_d in a single-path Rayleigh fading channel when C=1/2, $\gamma_{b,l}$=5 dB, T=1/19200 sec, N_a=9 and J=1920. It can be seen that the analytic results agree very well with the simulation result. It can be seen that, for a given m_l, $w_l(m_l)$ monotonically decreases as f_d increases until it reaches the minimum value and that the larger m_l, the faster $w_l(m_l)$ decreases. Comparing the correlation output with a given threshold η for all integer values of m_l, we can find $\hat{m}_l$ satisfying $w_l(\hat{m}_l) = \eta$. For example, $\hat{m}_l$ = 8, 16, 35, 76 and 166 for η=0.3 when f_d= 30, 70, 150, 325 and 650 Hz, respectively.

The optimum tap size can be represented as a function of $\hat{m}_l$ (refer to Appendix B)

$$\hat{N}_l = \left(\frac{16\hat{m}_l^4}{C\gamma_{b,l}S_l\beta^2\hat{f}_l^4} \cdot \frac{1+K_l}{K_l\cos^4\theta_l/9 + 1/\chi_l} \right)^{1/5} \tag{21}$$

where $\hat{f}_l$ is the normalized maximum Doppler frequency. Note that $\hat{f}_l$ is not a function of f_d but a function of other channel condition parameters.

It may not be effective to adjust the tap size in response to small variation of the channel parameters. In practice, it can be possible to determine the tap size considering the maximum and minimum values of the channel parameters. As an example, Fig. 3 depicts the upper and lower bound of the tap size as a function of $\hat{m}_l$ when the channel condition parameters (CCPs) are given as 0 (i.e., Rayleigh)$\le K_l < \infty$ (i.e., specular component only), $-90° \le \theta_l \le 90°$, 0 dB $\le \gamma_{b,l} \le$ 10 dB, $0.1 \le S_l \le 1$ and $24 \le \chi_l \le 45$. Rather than considering all the channel parameters independently, the channel condition is classified into a number of cases using a staircase approximation as shown in Fig. 3, where $m_{l,i}$ is $\hat{m}_l$ specified in the staircase.

Since $w_l(m)$ fast decreases as m increases as shown in Fig. 2, the channel condition can be classified by comparing $w_l(m)$ with a threshold η. If the j-th correlator output of the l-th branch becomes less than η for the first time, i.e.,

$$w_l(m_{l,j}) < \eta \text{ and } w_l(m_{l,j-1}) \ge \eta,\ j = 1, 2, \ldots, G_l \tag{22}$$

we infer that the channel condition belongs to the case-j. In this case, the tap size of the corresponding MA FIR filter is set to $N_{l,j}$, $1 \le j \le G_l$. Note that the tap size N_{l,G_l+1} corresponds to the case when no correlator output is less than

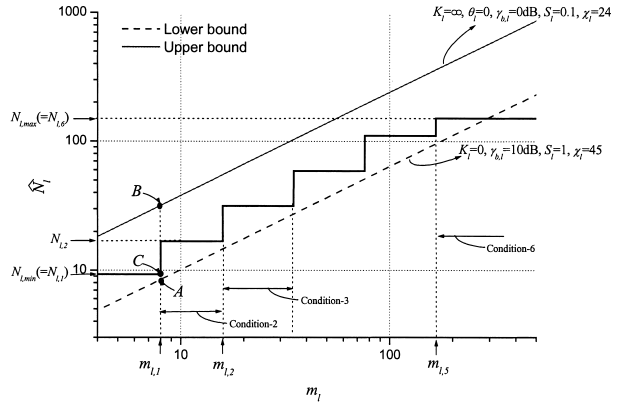

Fig. 3 Relation of the tap size and the correlation interval.

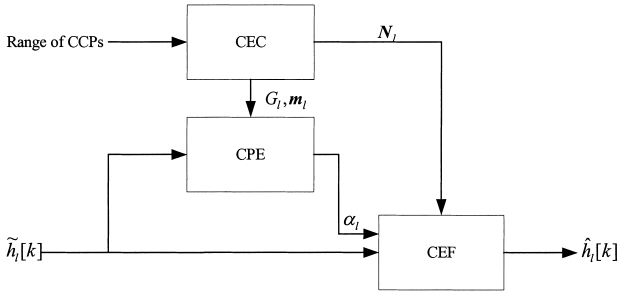

Fig. 4 Structure of the proposed ACE.

the threshold. This condition can occur when the channel response very slowly varies. In this case, it suffices to set the filter tap size to a pre-determined maximum value since the optimum tap size is not much changed due to the effect of the FPC as described before.

Figure 4 depicts the proposed ACE scheme of the l-th branch of the rake receiver. The proposed scheme consists of the CEF, channel parameter estimator (CPE) and the channel estimation controller (CEC). The CPE classifying the channel condition by (22), i.e., $\alpha_l = j$ is supplied to adjust the tap size of the MA FIR CEF. When the base station is initialized, the values of G_l, $m_{l,i}$ and $N_{l,i}$, i=1, 2, …, G_l, are determined using a staircase approximation in the CEC by considering the range of the channel condition parameters (CCPs). The CEC considers the minimum and maximum values of the CCPs, i.e., K_l, θ_l, S_l, $\gamma_{b,l}$ and χ_l, and other parameters such as η, N_a, $N_{l,min}$ and $N_{l,max}$. From these parameters, the upper and lower bound of the tap size can be determined using (21). Based on the minimum and maximum value of the CCPs, the magnitude $\boldsymbol{m}_l$ of the delay parameter and the tap size $\boldsymbol{N}_l$ of the CEF can be determined in a sequential manner. This process is described in Appendix C. Under the CCPs shown in Fig. 3, we can obtain G_l=5, $\boldsymbol{m}_l$={8, 16, 35, 76, 166} and $\boldsymbol{N}_l$={9, 17, 31, 57, 105, 150}. It suffices to update the tap size of the MA CEF once every J symbols time interval using (20). The channel condition can be estimated with an acceptable accuracy by correlating symbols less than a few thousands. When J=1920, the CEF can be updated for each 100 msec. Thus, the use of the proposed scheme is quite feasible even when the channel environment varies fast. Since the prefilter is used to remove the excess band noise, it suffices to have the bandwidth slightly larger than the allowable maximum Doppler frequency (750 Hz). Thus, we use a 9-tap MA FIR filter as the prefilter, i.e., N_a=9.

It is possible to use one-pole IIR filters as the CEF for further reduction of the implementation complexity with a small performance degradation [18]. The frequency response of an MA FIR filter can be approximated by that of one-pole IIR filter as [7]

$$\hat{h}_l[k] = \mu_l \hat{h}_l[k-1] + (1-\mu_l)\tilde{h}_l[k] \tag{23}$$

where $\mu_l = 1 - (\hat{N}_l/2 + 1)^{-1}$. Thus, the results obtained with the use of an MA FIR CEF can also be applied to the use of a one-pole IIR CEF.

5. Performance Evaluation

To investigate the effect of channel estimation on the receiver performance, the required E_b/I_0 is evaluated in multipath channels with a classic spectrum when the transmit signal power is fast controlled at a rate of 800 Hz. The PDR β^2 is set to 1/4 (i.e., −6 dB) by considering the trade-off between the pilot redundancy and the accuracy of the estimated CIR. Numerical results show that the proposed scheme operates well even when β^2 is small. The simulation condition is summarized in Table 1 and the range of CCPs is the same as that in Fig. 3. For performance comparison, we consider the use of 150-tap Wiener CEF [17]. Note that the performance improvement with the use of Wiener CEF with a tap size larger than 150 is negligible. We also consider the MA FIR CEFs with fixed tap size 24-tap and 96-tap corresponding to an average time of 1.25 msec or 5 msec, respectively. Note that the use of 24-tap MA FIR filter is effective for f_d of nearly up to 500 Hz and that the use of 96-tap MA FIR CEF is considered for low f_d.

Figure 5 depicts the required E_b/I_0 to provide 10^{-3} bit error rate (BER) under single-path and three-path channel condition. The use of 96-tap MA FIR CEF can provide BER performance similar to that of the optimum MA FIR CEF when f_d is low. As f_d increases, however, the averaging interval becomes larger than the optimum value. As a result, the BER performance with the use of 96-tap MA FIR CEF rapidly deteriorates as f_d increases. The use of 24-tap MA FIR CEF provides optimum performance only at f_d around 250 Hz. On the other hand, the optimum MA FIR CEF designed by (18) provides receiver performance similar to or slightly poorer than the Wiener CEF except at very high f_d. It can be seen that the performance difference between the two CEFs increases as f_d increases. This is mainly due to that the proposed MA FIR CEF uses a reduced tap size, while the Wiener CEF uses a fixed large tap size. It can also be seen that the proposed scheme can provide BER performance nearly the same as the use of the optimum MA FIR CEF over a wide range of f_d. For example, when f_d=5, 15, 50, 150, 300 and 500 Hz in three-path Rayleigh fading

Table 1 Simulation condition.

Parameters	Values
Data rate	9.6 Kbps
Chip rate	1.2288 Mcps
Spreading factor	64
Spreading sequence	m-sequence with a period of $2^{15}-1$
β^2	0.25
Channel coding	Convolutional (C=1/2 and H=9)
Interleaver	24x16 (20 ms)
Channel	Rayleigh and Ricean (Classic)
Multipaths	L=1 and 3 (equal average gain)
f_d	5–500 Hz
Power control	Step size=1 dB, control rate=800 Hz
Number of fingers	≤ 3
CPE parameters	J=1920,η=1/8,G_I=5,λ_L=0.15,λ_U=0.75

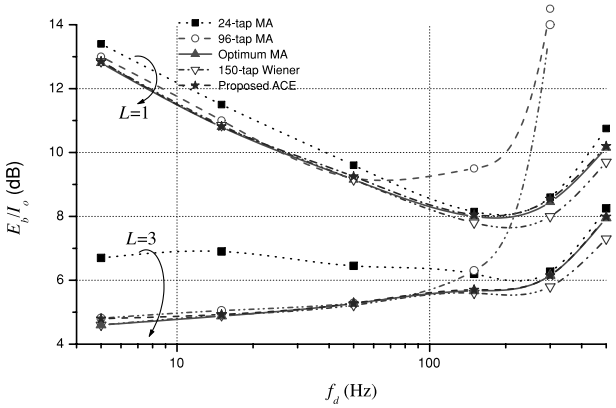

(a) Rayleigh ($K_l = 0$)

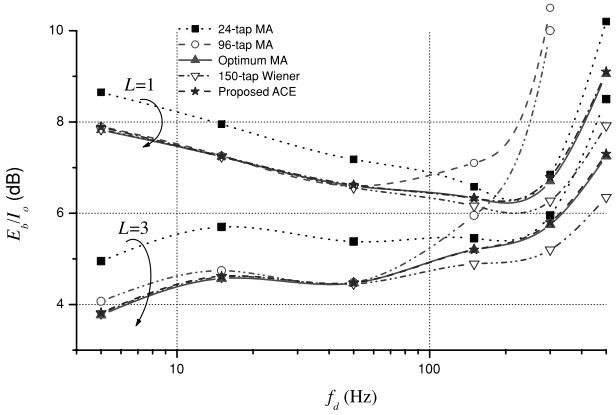

(b) Ricean ($K_l = 2$, $\theta_l = 0°$)

Fig. 5 Required E_b/I_0 at a BER of 10^{-3}.

channel, the proposed scheme uses MA CEF with the tap size of 150, 150, 105, 57, 31 and 17, respectively, while the optimum tap size is 806, 335, 129, 53, 30 and 20, respectively. Numerical results suggest that the use of an MA FIR filter is a good practical choice as the CEF considering the implementation complexity and performance. When the channel has multiple paths, the signal power will be split, reducing the received signal power in each finger of the rake receiver. In this case, the use of an efficient CEF becomes much important issue. Thus, the E_b/I_0 gain with the use of the proposed scheme increases as the number of paths increases.

The implementation complexity is compared in Table 2 in terms of the required memory and multiplication operation. Although additional memory is required by the proposed scheme for storage of pilot symbol, it is negligible. The proposed scheme requires the increase of the multiplication operation compared to the use of a fixed channel estimation scheme. However, it has computational complexity much less than other adaptive schemes with the use of CEF such as Wiener filter or general FIR filter. Thus, the proposed scheme can be realized in practice with an acceptable implementation complexity.

6. Conclusions

In this paper, we have considered the use of MA FIR filters as the CEF in DS-CDMA systems that transmit pilot signal in parallel with data signal. For a given channel condition, the tap size (i.e., bandwidth) of the MA FIR CEF is analytically designed to minimize the MSE of the channel estimate. We propose an ACE that adjusts the tap size of the MA FIR CEF in response to the variation of the channel condition in real time. For ease of implementation, the channel condition is classified into a small number of cases by exploiting the correlation properties of the received pilot signal. Numerical results show that the proposed ACE can provide near optimum performance for wide range of the channel condition, while significantly reducing the implementation complexity compared to the optimum Wiener CEF.

References

[1] F. Ling, "Coherent detection with reference symbol based channel estimation for direct sequence CDMA uplink communications," Proc. VTC'93, pp.400–403, May 1993.

[2] Y. Liu and S.D. Blostein, "Identification of frequency non-selective fading channels using decision feedback and adaptive liner prediction," IEEE Trans. Commun., vol.34, no.2/3/4, pp.1484–1492, Feb./March/April 1995.

[3] P.Y. Kam, "Adaptive diversity reception over a slow nonselective fading channel," IEEE Trans. Commun., vol.35, no.5, pp.572–574, May 1987.

[4] J.G. Proakis, Digital communications, 3rd ed. McGraw-Hill, 1995.

[5] M. Benthin and K. Kammeyer, "Influence of channel estimation on the performance of a coherent DS-CDMA system," IEEE Trans. Veh. Technol., vol.46, no.5, pp.262–268, May 1997.

[6] H. Andoh, M. Sawahashi, and F. Adachi, "Channel estimation filter using time-multiplexed pilot channel for coherent rake combining in DS-CDMA mobile radio," IEICE Trans. Commun., vol.E81-B, no.7, pp.1517–1526, July 1998.

[7] H.J. Oh and J.M. Cioffi, "An adaptive channel estimation scheme for DS-CDMA systems," Proc. VTC'2000 Fall, pp.2839–2843, Oct. 2000.

[8] M. Sakamoto, J. Huoponen, and I. Niva, "Adaptive channel estimator with velocity estimator for W-CDMA receiver," Proc. VTC'2000 Spring, pp.2024–2028, May 2000.

[9] G. Chen, X.-H. Yu, and J. Wang, "Adaptive channel estimation and dedicated pilot power adjustment based on the fading-rate measurement for a pilot-aided CDMA system," IEEE J. Sel. Areas Commun., vol.19, no.1, pp.132–140, Jan. 2001.

[10] 3GPP, 3G TS 25.211-Physical channels and mapping of transport channels onto physical channels (FDD), June 2001.

Table 2 Implementation complexity.

CE	Type	Memory	Memory (exam)	Multi./sec	Multi./sec (exam) ($\times 10^3$)
Fixed CE	General FIR	FN_f	450	FN_f/T	8640
	MA FIR	FN_f	450	F/T	57.6
	One-pole IIR	F	3	F/T	57.6
Proposed adaptive CE	MA FIR	FN_{max}	450	F/T	57.6
	One-pole IIR	F	3	F/T	57.6
	CPE	$F(m_{max}-N_{max})$	48	$\frac{F(G_l+1)+(FG_l)/J}{T}$	345.75

$*$. N_f(tap size of the fixed CPICH CEF)=150, N_{max}(maximum tap size of the adaptive CPICH CEF)=150, m_{max}(maximum correlator's interval)=166, J(correlation period)=1920 and F(number of fingers)=3.

[11] TIA, The cdma2000 ITU-R RTT candidate submission, June 1998.
[12] W.C. Jakes, Microwave mobile communications, John Wiley and Sons, 1974.
[13] K. Cheun, "Performance of direct-sequence spread-spectrum rake receivers with random spreading sequences," IEEE Trans. Commun., vol.45, no.9, pp.1130–1143, Sept. 1997.
[14] P. Schramm and R.R. Muller, "Pilot symbol assisted BPSK on Rayleigh fading channels with diversity: Performance analysis and parameter optimization," IEEE Trans. Commun., vol.46, no.12, pp.1560–1563, Dec. 1998.
[15] H. Hansen, S. Affes, and P. Mermelstein, "A Rayleigh Doppler frequency estimator derived from maximum likelihood theory," Proc. SPAWC'99, pp.382–386, April 1999.
[16] M. Hellebrandt, R. Mathar, and M. Scheibenbogen, "Estimating position and velocity of mobiles in a cellular radio network," IEEE Trans. Veh. Technol., vol.46, no.1, pp.65–71, Feb. 1997.
[17] M.D. Srinath, P.K. Rajasekaran, and R. Viswanathan, Statistical signal processing with applications, Prentice Hall, 1996.
[18] J.-W. Choi and Y.-H. Lee, "Adaptive channel estimation in DS-CDMA downlink systems," Proc. PIMRC'02, pp.1432–1436, Sept. 2002.

Appendix A: Derivation of the Optimum κ_l

The optimum κ_l minimizing the MSE can be obtained by

$$\begin{aligned}\left.\frac{\partial \varepsilon_l(\kappa_l)}{\partial \kappa_l}\right|_{\kappa_l=\hat{\kappa}_l} &= -\frac{1}{\hat{\kappa}_l^2}\int_0^{2\hat{\kappa}_l} R_{h,l}(t)dt + \frac{1}{\hat{\kappa}_l^3}\int_0^{2\hat{\kappa}_l} tR_{h,l}(t)dt \\ &\quad + \frac{2}{\hat{\kappa}_l^2}\int_0^{\hat{\kappa}_l} R_{h,l}(t)dt - \frac{2}{\hat{\kappa}_l}R_{h,l}(\hat{\kappa}_l) - \frac{T}{2\hat{\kappa}_l^2}\frac{\sigma_{n,l}^2}{\beta^2} \\ &= 0. \end{aligned} \tag{A·1}$$

Substituting the following Taylor approximations for $0 \le t \le 2\pi/3$ into (A·1),

$$\begin{aligned}\cos(t) &= \sum_{k=0}^{\infty}\frac{(-1)^k t^{2k}}{(2k)!} \approx 1 - \frac{t^2}{2!} + \frac{t^4}{4!} \\ J_0(t) &= \sum_{k=0}^{\infty}\frac{(-1)^k t^{2k}}{2^{2k}(k!)^2} \approx 1 - \frac{t^2}{4} + \frac{t^4}{64} \\ \frac{\sin(t)}{t} &= \sum_{k=0}^{\infty}\frac{(-1)^k t^{2k}}{(2k+1)!} \approx 1 - \frac{t^2}{3!} + \frac{t^4}{5!}\end{aligned} \tag{A·2}$$

$\hat{\kappa}_l$ can be represented as

$$\hat{\kappa}_l = \frac{1}{2}\left\{\frac{T\sigma_{n,l}^2}{(\pi f_d)^4\beta^2}\left(\frac{P_l\cos^4\theta_l}{9} + \frac{\sigma_{\alpha,l}^2}{\chi_l}\right)^{-1}\right\}^{1/5} \tag{A·3}$$

where χ_l is a constant equal to 24 and 45 in the case of the classic and flat spectrum, respectively.

Since the energy of the received signal per bit can be represented as

$$\begin{aligned}E_b &= \frac{T}{C}\sum_{l=0}^{L-1}(P_l + \sigma_{\alpha,l}^2) \\ &= \frac{N_0}{C\sigma_{n,l}^2}\sum_{l=0}^{L-1}(P_l + \sigma_{\alpha,l}^2)\end{aligned} \tag{A·4}$$

$\hat{\kappa}_l$ can be rewritten by

$$\hat{\kappa}_l = \frac{1}{2}\left\{\frac{T\sum_{i=0}^{L-1}(P_i + \sigma_{\alpha,i}^2)}{(\pi f_d)^4 C\gamma_{b,l}\beta^2}\left(\frac{P_l\cos^4\theta_l}{9} + \frac{\sigma_{\alpha,l}^2}{\chi_l}\right)^{-1}\right\}^{1/5} \tag{A·5}$$

where $\gamma_{b,l}$ is equal to $E_b/I_{0,l}$.

Appendix B: Derivation of (21)

Assuming that the prefiltered output $\bar{h}_l[n]$ is an egordic process and $m_l \ge N_a$, $w_l(m_l)$ can be approximated as [12]

$$\begin{aligned}w_l(m_l) &\simeq \frac{E\left\{\mathrm{Re}\left(\bar{h}_l^*[n]\bar{h}_l[n+m_l]\right)\right\}}{E\left\{\left|\bar{h}_l[n]\right|^2\right\}} \\ &= \frac{P_l\cos(2\pi f_d m_l T\cos\theta_l) + \sigma_{\alpha,l}^2 R_{\alpha,l}(m_l T)}{P_l + \sigma_{\alpha,l}^2 + P_N}\end{aligned} \tag{A·6}$$

The power of the prefiltered noise is given by

$$P_N = \frac{\sigma_{n,l}^2}{\beta^2 N_a} = \frac{1}{\beta^2 N_a C\gamma_{b,l}}\sum_{i=0}^{L-1}(P_i + \sigma_{\alpha,i}^2). \tag{A·7}$$

Let $\hat{f}_l$ be the normalized maximum Doppler frequency,

$$\hat{f}_l = 2\pi f_d \hat{m}_l T \tag{A·8}$$

where $w_l(\hat{m}_l) = \eta$. Substituting (A·2) into (A·6), it can be

shown that

$$a_l \hat{f}_l^4 - b_l \hat{f}^2 + c_l = 0 \quad (\text{A}\cdot 9)$$

where

$$a_l = \begin{cases} \frac{P_l \cos^4\theta_l}{24} + \frac{\sigma_{\alpha,l}^2}{64}, \ Classic \\ \frac{P_l \cos^4\theta_l}{24} + \frac{\sigma_{\alpha,l}^2}{120}, \ Flat \end{cases}$$

$$b_l = \begin{cases} \frac{P_l \cos^2\theta_l}{2} + \frac{\sigma_{\alpha,l}^2}{4}, \ Classic \\ \frac{P_l \cos^2\theta_l}{2} + \frac{\sigma_{\alpha,l}^2}{6}, \ Flat \end{cases}$$

$$c_l = (1-\eta)(P_l + \sigma_{\alpha,l}^2) - \eta P_N. \quad (\text{A}\cdot 10)$$

Thus, $\hat{f}_l$ is determined by

$$\hat{f}_l = \left(\frac{b_l - \sqrt{b_l^2 - 4a_l c_l}}{2a_l} \right)^{1/2}. \quad (\text{A}\cdot 11)$$

Note that $\hat{f}_l$ is not a function of f_d and depends upon other channel condition parameters. Using $2\pi f_d T = \hat{m}_l^{-1} \hat{f}_l$, the optimum filter tap size $\hat{N}_l$ can be rewritten as a function of $\hat{m}_l$ as

$$\hat{N}_l = \left(\frac{2^4 \hat{m}_l^4}{C\gamma_{b,l} S_l \beta^2 \hat{f}_l^4} \cdot \frac{1+K_l}{K_l \cos^4\theta_l/9 + 1/\chi_l} \right)^{1/5}. \quad (\text{A}\cdot 12)$$

Appendix C: Decision of the CPE Parameters

The lower bound of the filter tap size is obtained by substituting the parameters $S_{l,\max}$, $\chi_{l,\max}$, $K_{l,\min}$, $|\theta_l|_{\max}$, $\beta_{\max}$ and $\gamma_{b,l,max}$ into (21). Similarly, the upper boundary of the filter tap size is obtained by the value of $S_{l,\min}$, $\chi_{l,\min}$, $K_{l,\max}$, $|\theta_l|_{\min}$, $\beta_{\min}$ and $\gamma_{b,l,min}$, where the subscript 'max' and 'min' respectively denote the maximum and minimum values of the parameter.

The tap size of the first CEF $N_{l,1}$ is set to a minimum tap size $N_{l,min}$. Then, the value of $m_{l,1}$ is determined from $N_{l,1}$. Let us introduce the lower bound margin factor λ_L and the upper bound margin factor λ_U ($0 \le \lambda_L, \lambda_U < 1$) to have a freedom in the design of the CPE. λ_L is determined such that the point A in Fig. 3 is represented as $(m_{l,1}, N_{l,1}/(1+\lambda_L))$. It can be shown that, for $1 \le i \le G_l$,

$$m_{l,i} = \left\{ \frac{CN_{l,i}^5 \hat{f}_{l,\max}^4 \left(\frac{K_{l,\min}\cos^4|\theta_l|_{\max}}{9} + \chi_{l,\max}^{-1} \right)}{16\gamma_{b,l,\max}^{-1} S_{l,\max}^{-1} \beta_{\max}^{-2} (1+\lambda_L)^5 (1+K_{l,\min})} \right\}^{1/4}. \quad (\text{A}\cdot 13)$$

As λ_L increases, the difference between the break points of the staircase shape (e.g., the point C in Fig. 3) and the lower bound becomes larger. With λ_U and $m_{l,1}$, the tap size $N_{l,2}$ of the second CEF in the l-th finger is determined such that $(m_{l,1}, (1+\lambda_U)N_{l,2})$ is on the upper bound (e.g., the point B in Fig. 3). It can be shown that, for $1 \le i \le G_l$,

$$N_{l,i+1} = \frac{1}{1+\lambda_U} \cdot \left\{ \frac{16\hat{f}_{l,\min}^{-4} S_{l,\min}^{-1} \beta_{\min}^{-2} m_{l,i}^4 (1+K_{l,\max})}{C\gamma_{b,l,\min}\left(\frac{K_{l,\max}\cos^4|\theta_l|_{\min}}{9} + \chi_{l,\min}^{-1} \right)} \right\}^{1/5}. \quad (\text{A}\cdot 14)$$

Similarly, $m_{l,2}$ can be calculated from $N_{l,2}$ and (A· 13) with i=2. Thus, $N_{l,3}$ can be calculated from $m_{l,2}$ and (A· 14) with i=2. In this way, $m_{l,i}$, i=1, 2,$\cdots$, G_l, and $N_{l,i}$, i=1, 2,$\cdots$, G_l+1, can be determined in a sequential manner until the tap size becomes larger than the predetermined maximum value $N_{l,max}$. When $N_{l,i+1} \ge N_{l,max}$, $N_{l,i+1}$ is set to a value of $N_{l,max}$.

In order to uniquely design the proposed ACE, we need to determine η, λ_L, λ_U, $N_{l,min}$, $N_{l,max}$ and the minimum and the maximum values of the CCPs. The threshold η can be set to any positive value less than one since η is already considered in the design of ACE by determining c_l in (A· 10). If the channel has a large number of multipaths, the signal power is split into multiple paths. This effectively increases the denominator of (A· 6), reducing the maximum value of the autocorrelation. Thus, it is desirable to set the threshold to a small positive value.

It is possible to increase the design freedom by adjusting the tap margin factor λ_L and λ_U. The bandwidth of an MA FIR filter decreases as the tap size increases. If the filter tap size is smaller than the desired one, the output may suffer from excessive noise. On the other hand, when the tap size is much larger than the optimum one, the desired information can be filtered out, resulting in severe performance degradation in channel estimation. Therefore, it is desirable to determine the tap margins so that $0 \le \lambda_L < \lambda_U < 1$ for conservative design.

The minimum tap size $N_{l,min}$ should be determined so that the receiver can operate even in the worst case (e.g., up to an allowable maximum Doppler frequency). In order to obtain near optimum performance in a very slow fading channel, the maximum tap size $N_{l,max}$ should be determined so that the use of a CEF with a tap size larger than $N_{l,max}$ can provide negligible performance improvement over the use of $N_{l,max}$-tap MA FIR CEF. However, $N_{l,max}$ does not have to be very large because the optimum tap size is not much affected by low f_d due to the effect of fast power control.

The range of the CCPs can significantly vary depending on the characteristics of the service condition such as the geometry and channel environment. For example, the maximum value of the Ricean factor K_l is set to a small value close to zero when the channel has no line-of-sight such as in urban area. If we know the characteristics of the service condition, we can constrict the range of the CCPs, reducing the difference between the lower and upper bound of the tap size. The smaller the difference, the better the accuracy of the channel information can be obtained. When there is no exact a priori information on the channel environment such as the fading characteristics and the SIR of the received signal, the proposed scheme can be designed with a set of the CCPs for a presumed nominal operating condition as given

in Fig. 3.

Ji-Woong Choi received the B.S. and M.S. degree in electrical engineering from Seoul National University, Korea, in 1998 and 2000, respectively. He is now working toward the Ph.D. degree in electrical engineering from Seoul National University, Korea. His research areas are wireless transmission systems including spread spectrum and OFDM systems, and signal processing for communication systems.

Yong-Hwan Lee received the B.S. degree from Seoul National University, Korea, in 1977, the M.S. degree from the Korea Advanced Institute of Science and Technology (KAIST), Korea, in 1980, and the Ph.D. degree from the University of Massachusetts, Amherst, U.S.A., in 1989, all in electrical engineering. From 1980 to 1985, he was with the Korea Agency for Defense Development, where he was involved in development of shipboard weapon fire control systems. From 1989 to 1994, he worked for Motorola as a Principal Engineer, where he was engaged in research and development of data transmission systems including high-speed modems. Since 1994, he has been with the School of Electrical Engineering and Computer Science, Seoul National University, Korea, as a faculty member. His research areas are wired/wireless transmission systems including spread spectrum systems, robust signal detection/estimation theory and signal processing for communications.